

UNCLASSIFIED

~~RESTRICTED~~

COPY NO. 100

RM No. E6K29

JPL LIBRARY
CALIFORNIA INSTITUTE OF TECHNOLOGY

Classification Changed to
UNCLASSIFIED

Authority
DOD DIR 5200.10

Date
10-31-64

By
A. Mohu

NACA

GROUP 4

Downgraded at 3 year
intervals; declassified
after 12 years

RESEARCH MEMORANDUM

JET DIFFUSER FOR SIMULATING RAM CONDITIONS ON A
TURBOJET-ENGINE STATIC TEST STAND

By H. R. Bohanon, David S. Gabriel
and Robert H. Essig

Aircraft Engine Research Laboratory
Cleveland, Ohio

**CASE FILE
COPY**

CLASSIFIED DOCUMENT

This document contains classified information affecting the National Defense of the United States within the meaning of the Espionage Act, USC 50:31 and 32. Its transmission or the revelation of its contents in any manner to an unauthorized person is prohibited by law. Information so classified may be imparted only to persons in the military and naval Services of the United States, appropriate civilian officers and employees of the Federal Government who have a legitimate interest therein, and to United States citizens of known loyalty and discretion who of necessity must be informed thereof.

TECHNICAL
EDITING
WAIVED

**NATIONAL ADVISORY COMMITTEE
FOR AERONAUTICS**

WASHINGTON

January 28, 1947

~~RESTRICTED~~
UNCLASSIFIED

~~RESTRICTED~~
UNCLASSIFIED

NATIONAL ADVISORY COMMITTEE FOR AERONAUTICS

RESEARCH MEMORANDUMJET DIFFUSER FOR SIMULATING RAM CONDITIONS ON A
TURBOJET-ENGINE STATIC TEST STANDBy H. R. Bohanon, David S. Gabriel
and Robert H. Essig

SUMMARY

A jet diffuser for simulating flight or ram conditions on a turbojet-engine static test stand was designed and investigated. The diffuser utilizes the kinetic energy of the jet from a turbojet engine to reduce the discharge pressure at the exhaust nozzle and thereby provides simulated ram-pressure ratios across the engine. The engine exhaust nozzle discharges into an exhaust chamber (flexibly sealed to the tail pipe), which is connected to a diffuser by a bell-shaped nozzle. The pressure in the exhaust chamber is controlled independently of engine speed by a variable-area shutter at the diffuser discharge.

The jet diffuser simulated ram-pressure ratios from 0.95 to 2.2 at various simulated pressure altitudes for a range of engine speeds from 85 to 100 percent of maximum rpm. Agreement of data obtained with and without the jet diffuser for a ram-pressure ratio of 1.0 indicated that the presence of the diffuser did not interfere with the flow through the engine exhaust-nozzle outlet.

INTRODUCTION

Two of the basic factors affecting the performance characteristics of turbojet engines are altitude and ram-pressure ratio (ratio of the compressor-inlet total pressure to the ambient atmospheric pressure). The performance variation of turbojet engines with altitude at various ambient pressures and temperatures for a ram-pressure ratio of 1.0 can be accurately predicted from the results of sea-level static investigations. The effect of ram-pressure ratio, however, cannot be accurately evaluated from the results of an investigation on a static test stand. Consequently, it has been necessary to resort to either wind-tunnel or flight studies to determine the performance of turbojet engines under ram conditions.

~~RESTRICTED~~
UNCLASSIFIED

A jet diffuser, which could be used to simulate ram conditions on a static test stand, was developed at the NACA Cleveland laboratory to reduce the extensive amount of equipment required for runs under ram or flight conditions. A description of the jet diffuser and the method of its installation on a conventional turbojet engine is presented. The use of the diffuser is illustrated by engine performance data obtained over a range of engine rotor speeds and for ram-pressure ratios from 0.95 to 2.2.

JET DIFFUSER

The jet diffuser utilizes the kinetic energy of the exhaust jet from the turbojet engine to decrease the engine back pressure and thereby to create a pressure ratio across the engine that simulates a ram-pressure rise at the compressor inlet. Because the engine exhausts into a pressure lower than sea-level atmospheric, the simulated ram-pressure ratio is obtained at some simulated altitude. The performance at the various simulated pressure altitudes resulting from the decreased exhaust-nozzle-outlet pressures can be correlated by plotting the results in terms of the generalized parameters; hence, the effects of ram-pressure ratio and altitude on performance may be separated.

As shown in the dimensioned sketch of figure 1, the jet diffuser, designed for use on an I-16 engine, consists of a cylindrical exhaust chamber, a bell-shaped nozzle, and a diffuser section followed by a 4-foot straight duct that is fitted with a conical target and a movable sleeve-type shutter. The conical target and movable-shutter arrangement were used to adjust the exhaust-chamber pressure and the ram-pressure ratio across the engine independently of the engine speed. A hydraulically operated piston with a 12-inch stroke was used to change the shutter position. The sleeve-type shutter assembly, which moved parallel to the diffuser axis, was used to eliminate the forces other than friction acting on the control valve and the saw-toothed edge of the shutter permitted fine adjustment of the exhaust-chamber pressure. The diffuser section, which has a throat area of 143 square inches ($13\frac{1}{2}$ -in. diameter), was constructed with a 7° total angle of diffusion and provided an area ratio of 3.4 in the 93-inch length. The exhaust chamber at the entrance to the jet diffuser provided a region for free expansion of the exhaust jet at supersonic velocities, thus permitting the accurate reproduction of engine performance without interference of the diffuser with the jet. The exhaust chamber also functioned as a plenum chamber and permitted accurate measurement of the static pressure at the exhaust-nozzle outlet.

The entire diffuser assembly was mounted on a movable frame as shown in the photograph of figure 2. This movable diffuser frame provided a means of adjusting the diffuser position with respect to the exhaust-nozzle outlet, which, for this investigation, was located approximately $8\frac{3}{4}$ inches from the diffuser throat (fig. 1).

During the runs, the diffuser frame was rigidly bolted to the test-cell apron and the exhaust chamber was flexibly connected to the engine by a clamped rubber diaphragm to prevent leakage, as shown in detail B, figure 3. A radiation shield was installed inside the exhaust chamber to protect the diaphragm from damage by heat, both inner and outer clamping flanges were cooled by water coils, and a water spray was directed against the outside face of the diaphragm.

APPARATUS

Installation. - The investigation of jet-diffuser performance was conducted on an I-16 turbojet engine. Figure 3 is a schematic diagram of the setup showing the test cell, the engine mounting frame and thrust-device linkage, and the jet diffuser. The engine was mounted on a rigid frame, which was freely suspended from the cell roof by four ball-bearing pivoted rods. Lateral movement of the engine frame was prevented by ball-bearing guide rollers. The tail pipe, which was fitted with a $12\frac{1}{2}$ -inch exhaust nozzle, extended through an air seal (detail A, fig. 3) in the outer cell wall.

Instrumentation. - The thrust forces produced by the engine were indicated by the measured pressures in a calibrated balanced-diaphragm air cell (reference 1), which was connected to the engine frame by means of a bell-crank linkage. Details of the thrust calibration are subsequently discussed. All supply lines and instrument connections to the engine were flexible in order that the restraining forces on the free-swinging frame would be at a minimum.

Engine fuel (kerosene) flow was measured with a calibrated rotameter and engine rotor speed was measured with a chronometric tachometer.

The air supply to the engine entered the nearly air-tight test cell through a standard A.S.M.E. air-metering nozzle with a throat diameter of 18 inches (fig. 3). An air-supply diffuser,

which has an area ratio of 4, was connected to the A.S.M.E. nozzle in order to convert the velocity pressure at the nozzle throat to static pressure in the test cell.

The following instrumentation, the location of which is shown in figures 1 and 3, was used to measure pressure and temperature:

- (a) Compressor-inlet air temperature T_1 , average of eight open-type thermocouples on inlet-air screens.
- (b) Compressor-inlet total pressure P_1 , one open-end tube in test cell.
- (c) Compressor-outlet total pressure P_2 , average of seven tubes in total-head rake located across inlet to burner 3.
- (d) Tail-pipe indicated gas temperature T_7 , average of four strut-type thermocouples located in tail pipe 8 inches upstream of exhaust nozzle and 90° apart.
- (e) Tail-pipe static pressure P_7 , piezometer ring with four common taps.
- (f) Exhaust-chamber static pressure P_8 , piezometer ring with four wall taps equally spaced around exhaust-chamber wall approximately in plane of engine exhaust-nozzle outlet. The reading of the piezometer ring was independently checked with a single exhaust-chamber wall tap connected to a separate manometer. This pressure corresponds to simulated-altitude ambient pressure.
- (g) Static pressures at various locations along jet diffuser p_9 to p_{15} (fig. 1).

PROCEDURE

Brief preliminary studies were first conducted to determine a suitable diffuser-throat size. With a diffuser-throat diameter of $12\frac{1}{2}$ inches (same diameter as exhaust-nozzle outlet) choking occurred at an indicated engine speed of about 15,500 rpm and limited the minimum pressure obtainable in the exhaust chamber. In order to prevent choking at this low engine speed and hence increase the range of ram-pressure ratios available, the throat diameter was increased to $13\frac{1}{2}$ inches ($16\frac{1}{2}$ percent greater area than the area of

the engine exhaust-nozzle outlet). With this increased throat diameter, no choking occurred until an indicated engine speed of 16,350 rpm (rated speed 16,500 rpm) was reached; the corrected engine speed was about 500 rpm less than the indicated speed because of the high compressor-inlet temperatures. The $13\frac{1}{2}$ -inch-diameter throat, which provided a wider range of available ram-pressure ratios, was used for the performance evaluation.

Engine runs were made over a range of rotor speeds from 14,000 to 16,500 rpm (85 to 100 percent of maximum rpm) for six diffuser-outlet shutter positions. Shutter positions are designated A to F, where A is the full-open position (maximum ram-pressure ratio) and F is the nearly closed position (negative ram-pressure ratio). The various shutter positions were arbitrarily chosen to divide the maximum vacuum obtained in the exhaust chamber at rated engine speed into approximately equal increments.

Runs were also made with the diffuser detached to establish standard performance at a ram-pressure ratio of 1.0.

METHOD OF CORRECTION OF ENGINE PERFORMANCE DATA

The following symbols are used in this report:

F_j	exhaust-jet thrust (total mass flow of exhaust gas times effective exhaust-jet velocity), (lb)
N	rotor speed, (rpm)
P	total pressure, (lb/sq in. absolute)
p	static pressure, (lb/sq in. absolute)
T	indicated gas temperature, ($^{\circ}$ R)
W_a	air flow, (lb/sec)
W_f	fuel flow, (lb/hr)

Subscripts:

1	compressor inlet
2	compressor outlet

7 tail pipe

8 exhaust chamber at nozzle outlet

9 to 15 various locations along jet diffuser

Because the effective diaphragm area was large, the forces on the engine due to the difference between the exhaust-chamber pressure and atmospheric pressure were large compared to the thrust forces. The correction for the forces contributed by this pressure differential was determined in the following manner: The engine tail pipe and the diffuser outlet were blanked off and the exhaust chamber was evacuated by means of a vacuum pump. The thrust-measuring device was then read for various pressure differences between the test cell and the exhaust chamber with zero gas flow through the engine. This thrust was plotted against the pressure difference between the test cell and the exhaust chamber. In any engine run, the thrust corresponding to the pressure difference between the test cell and the exhaust chamber was obtained from this curve and added to the thrust measured during the run to obtain the true jet thrust. In order to assure that the exhaust-chamber pressure p_g used in the calibration was the same as the effective pressure on the diaphragm seal during a test run, several static-pressure surveys were made in the exhaust chamber during subsequent engine runs. These surveys were made radially across the flexible diaphragm seal and longitudinally along the exhaust-chamber wall and along the engine exhaust-nozzle wall. The variation of individual static pressures was less than 0.05 pound per square inch and no pressure gradients were found that could appreciably effect the measured engine thrust.

Because of the low velocity at the engine inlet, this true jet thrust represents the thrust of the exhaust jet only, that is, the product of the mass of exhaust gas by the effective exhaust-jet velocity. The product of the mass flow of air into the engine and the airplane speed is subtracted from the jet thrust to compute the net thrust for flight conditions.

The following two conventional factors, which were used to correct the engine performance data to standard conditions, provide a means of correlating altitude performance data:

$\delta = \frac{\text{exhaust-nozzle-outlet static pressure, } p_g, \text{ (lb/sq in. absolute)}}{\text{NACA standard sea-level pressure}}$

$\theta = \frac{\text{compressor-inlet temperature, } T_1, \text{ (}^{\circ}\text{R)}}{\text{NACA standard sea-level temperature}}$

In some performance investigations of turbojet engines, the compressor-inlet total pressure rather than the exhaust static pressure is used in defining δ . It is emphasized that, in the definition of δ , the exhaust-nozzle-cutlet static pressure refers to the ambient exhaust static pressure, and not the static pressure in the jet near the nozzle throat. In the case of an engine in a flight installation, this corresponds to the static atmospheric pressure. The definition of δ based on the exhaust static pressure is used because a more complete separation of the effects of ram and altitude is effected and because this pressure is more convenient to apply.

The performance data at various altitudes are correlated by plotting the results in terms of the following generalized parameters:

F_j/δ	corrected jet thrust
$N/\sqrt{\theta}$	corrected engine speed
P/δ	corrected total pressure
p/δ	corrected static pressure
T/θ	corrected temperature
$W_a \sqrt{\theta}/\delta$	corrected air flow
$W_f/\delta \sqrt{\theta}$	corrected fuel flow

RESULTS AND DISCUSSION

The variation of exhaust-nozzle-outlet pressure with corrected engine speed for shutter positions A to F is shown in figure 4. These curves illustrate the range of nozzle-outlet pressures, hence the ram-pressure ratios, obtained over a range of engine speeds. The exhaust-nozzle-outlet absolute pressure decreases with an increase in engine speed for shutter positions A to E and increases at each constant engine speed as the shutter is closed (positions A to F). With the diffuser shutter full open (position A), the exhaust-nozzle-outlet pressure reaches a value of 12.9 inches of mercury absolute (corresponding to a ram-pressure ratio of 2.25 at a standard altitude of about 21,500 ft) at a maximum corrected engine speed of about 15,940 rpm. The minimum exhaust-nozzle-outlet pressure occurred at a corrected engine speed

of about 15,750 rpm indicating that choking occurred in the diffuser throat. The dashed portion of the curve for shutter position A indicates that data for this portion of the curve were not obtained; however, in preliminary studies the pressure varied in the manner shown whenever choking was encountered. Because of the variation of exhaust-nozzle-outlet pressure with engine speed, the minimum exhaust pressure or maximum ram-pressure ratio could be obtained only at maximum engine speed and, consequently, the range of engine speeds is limited at high ram-pressure ratios.

A typical pressure-distribution curve along the diffuser is shown in figure 5 for a corrected engine speed of 15,940 rpm and full-open shutter. The dashed line between the first two points indicates that the manner of variation in pressure between the engine nozzle outlet and the diffuser throat was not obtained.

Evidence of the presence of supersonic jet velocities was noted during the runs when a sudden change in the sound, from a deep rumble to a high-pitched scream, occurred at a corrected engine speed of about 15,000 rpm. The curve of figure 6 shows the variation in pressure ratio across the engine nozzle (the ratio of the tail-pipe inlet total pressure P_7 to exhaust-chamber-outlet static pressure P_8 , where the inlet total pressure is calculated from the measured static pressure p_7 , tail-pipe total temperature T_7 , and air flow) with corrected engine speed for runs with the diffuser shutter full open. This figure shows that the critical pressure ratio (about 1.9) occurs at the same corrected engine speed (15,000 rpm) as the sound change. The peak in the curve at an engine speed of about 15,750 rpm indicates the choking point of the diffuser previously mentioned in the discussion of figure 4.

The use of the jet diffuser for simulating ram conditions is illustrated by figures 7 to 11, which show the corrected performance of the engine plotted against ram-pressure ratio for various corrected engine speeds. The corrected performance parameters plotted are jet thrust, air flow, fuel flow, tail-pipe gas temperature, and compressor-outlet total pressure. The data were corrected for slight experimental differences in engine speed by plotting the rough data of engine performance against speed for various ram-pressure ratios and using the slope of the curves at various engine speeds to determine a correction factor. The curves of jet thrust do not include the drag created by the inlet air, which must be deducted to obtain net thrust. A scatter of the thrust data is evident in figure 7 at low engine speeds. This scatter is attributed to small uncertainties in evaluating the large forces contributed by

the difference between atmospheric and exhaust-chamber pressures acting on the exhaust-chamber diaphragm. These large forces could be reduced by using a sliding seal around the tail pipe; precautions must be taken, however, to eliminate leakage. Calibration of the thrust forces imposed by the pressures acting on the seal may be avoided by using a tail-pipe pressure rake to obtain engine thrust.

The correction factors θ and δ used to generalize the performance variables in figures 7 to 11 do not take into account any changes that may occur in the combustion efficiency. Therefore, extrapolation of the test results involving the fuel consumption of the engine to high altitudes may be unreliable. The variation of combustion efficiencies, and hence the error of the correlation, may be expected to be small at low altitudes but would increase as the burner critical altitude is approached.

Faired cross plots of figures 7 to 11 are shown in figures 12 to 16 in which the corrected engine performance is shown as a function of the corrected engine speed for various ram-pressure ratios from 0.95 to 2.2. The limited range of engine speeds at ram-pressure ratios above about 1.4 is evident from these curves. The points on each figure, which are performance-data points at a ram-pressure ratio of 1.0 taken without the jet diffuser, show good agreement with the cross-plotted curves. This agreement indicates that the jet diffuser does not interfere with the flow through the engine exhaust nozzle at a ram-pressure ratio of 1.0. At ram-pressure ratios high enough to produce critical pressure ratios across the engine exhaust nozzle, it is reasonable to expect that the presence of the diffuser walls will not influence the flow through the exhaust nozzle because no pressure disturbances downstream of the nozzle could be transmitted upstream past the nozzle outlet. Inasmuch as no interference effects were found at the very low ram-pressure ratio (1.0) and, as reasonable assurance exists that no interference is present at the very high ram-pressure ratios, performance is probably accurately obtained at intermediate values of ram-pressure ratio.

In order to check the accuracy of the performance data obtained with the jet diffuser, the experimental variation of thrust with ram-pressure ratio obtained from the diffuser runs is compared in figure 17 with the theoretically calculated variation obtained from the manufacturer for a similar turbojet engine. Although the magnitude of thrust is not the same (because of the present variation in performance of different engines of the same model), the agreement between the slopes of the curves is further verification of the accuracy of the performance obtained with the jet diffuser.

CONCLUSIONS

A jet diffuser, which was developed for use in simulating ram conditions for tests of a turbojet engine on a static test stand, produced a minimum exhaust-nozzle-outlet pressure of 12.9 inches of mercury absolute (corresponding to ram-pressure ratio of 2.25) at the maximum speed of an I-16 turbojet engine. A movable shutter on the diffuser outlet controlled the exhaust-nozzle-outlet pressure independently of engine speed to obtain the engine performance at ram-pressure ratios from 0.95 to 2.2 for a range of engine speeds from 85 to 100 percent of maximum rpm. The good agreement of performance data at a ram-pressure ratio of 1.0 taken with and without the diffuser indicated that the flow through the engine exhaust nozzle was not effected by the presence of the jet diffuser at this ram-pressure ratio.

Aircraft Engine Research Laboratory,
National Advisory Committee for Aeronautics,
Cleveland, Ohio.

REFERENCE

1. Moore, Charles S., Biermann, Arnold E., and Voss, Fred: The NACA Balanced-Diaphragm Dynamometer-Torque Indicator. NACA RB No. 4C28, 1944.

NACA RM No. E6K29

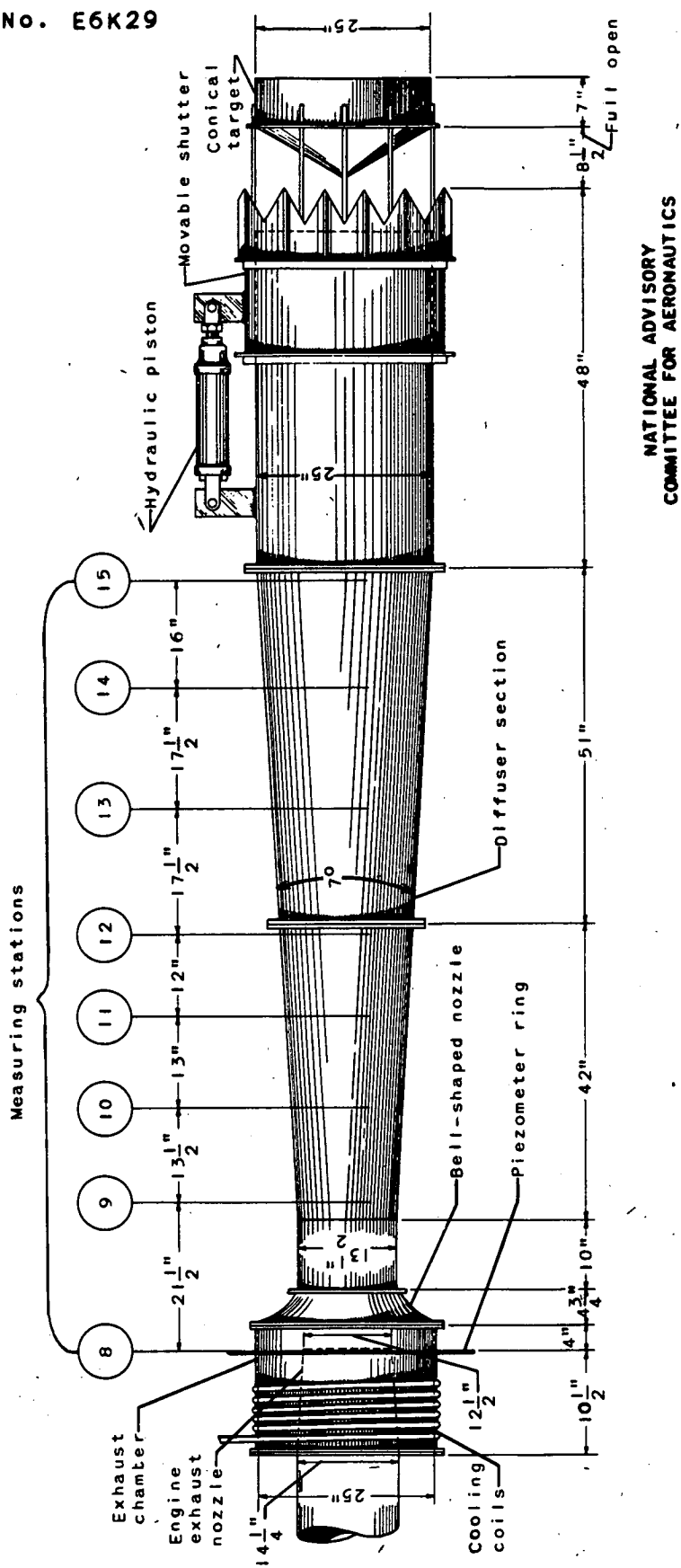


Figure 1. - Sketch of jet-diffuser assembly for 1-16 engine showing location of pressure taps.

NACA RM No. E6K29

Fig. 2

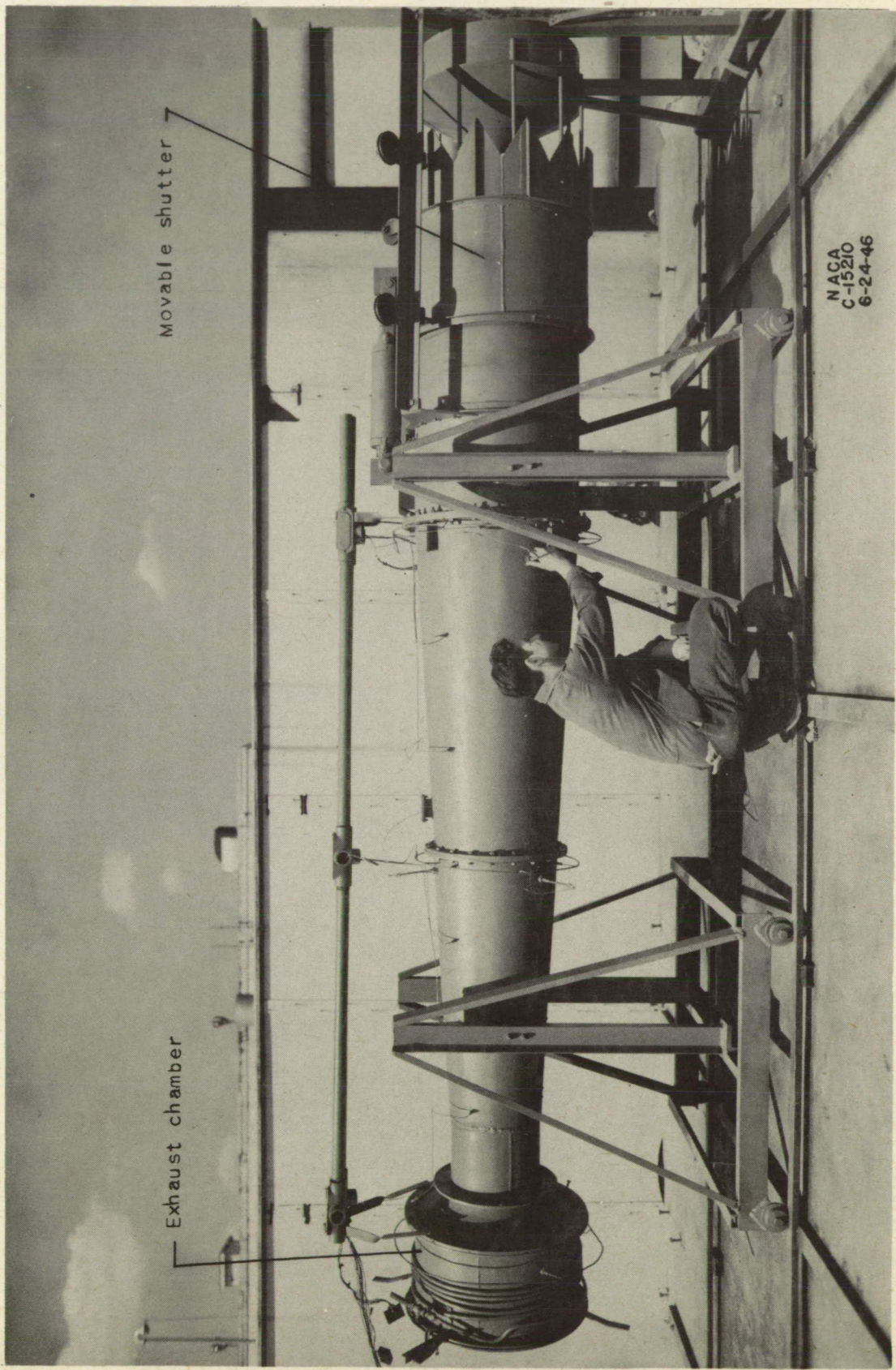


Figure 2. - Photograph of jet diffuser showing exhaust chamber and movable shutter.

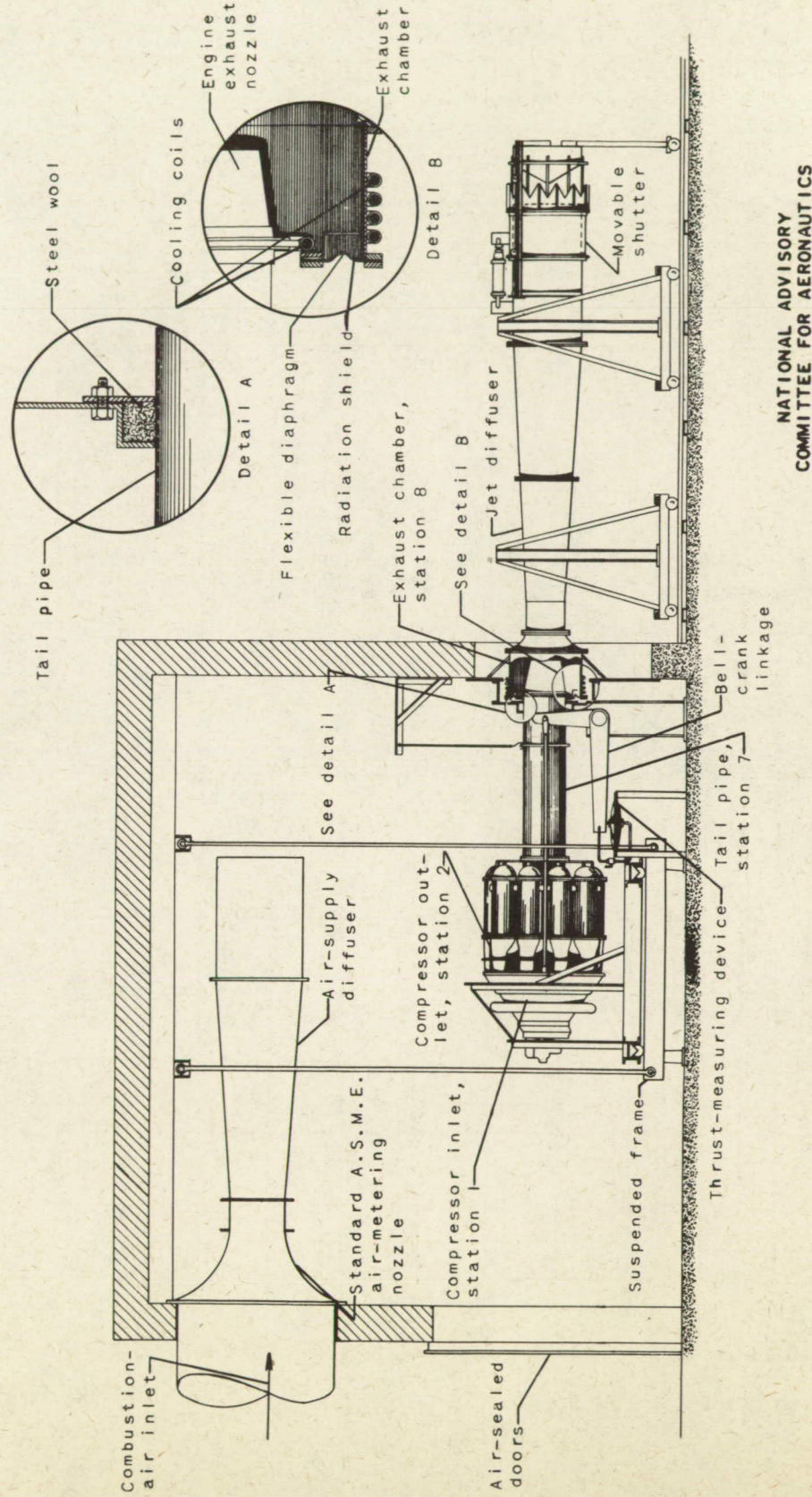


Figure 3. — Schematic diagram of apparatus for jet-diffuser investigation.

Fig. 4

NACA RM No. E6K29

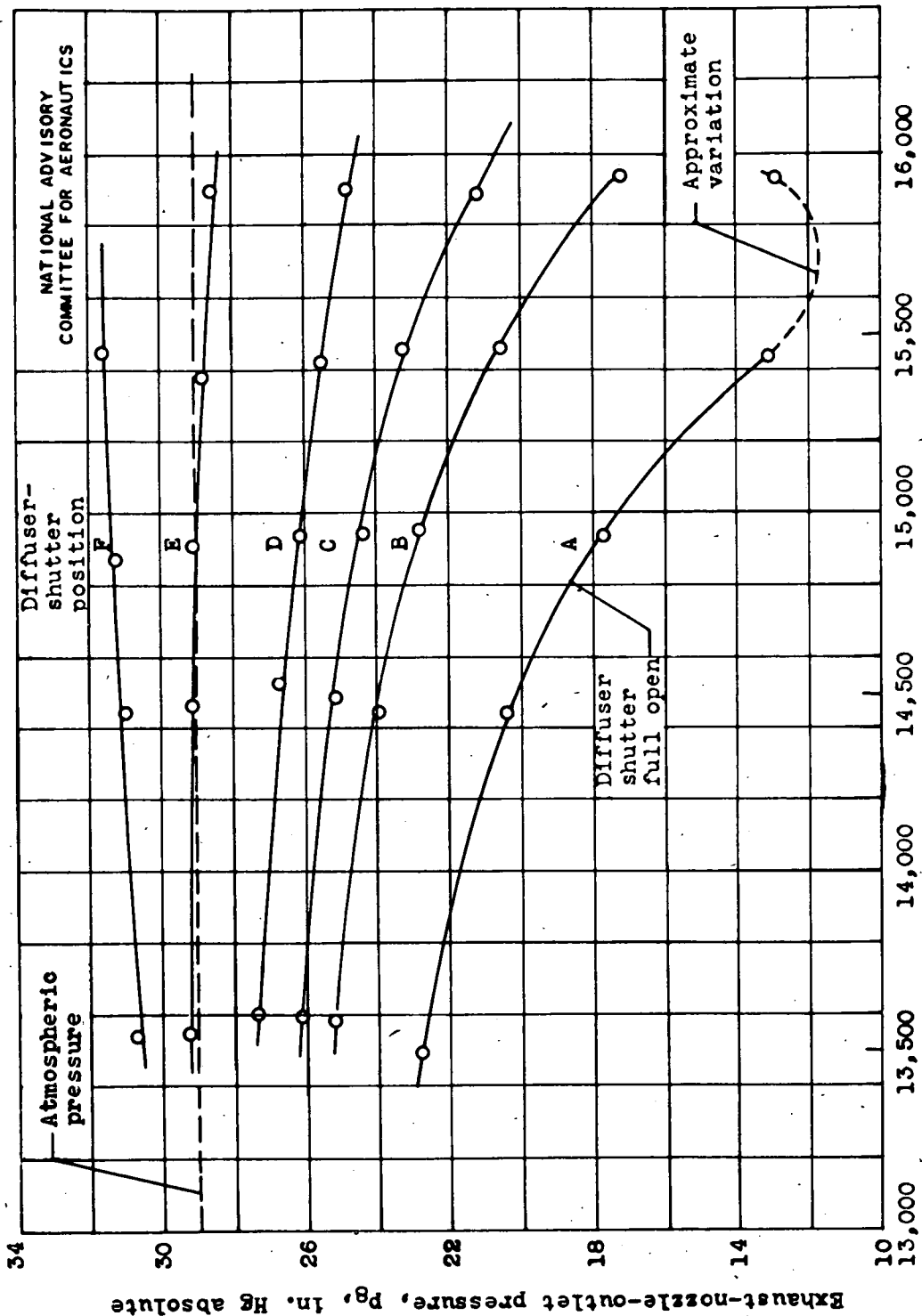


Figure 4. — Variation of exhaust-nozzle-outlet pressure with corrected engine speed for various shutter positions.

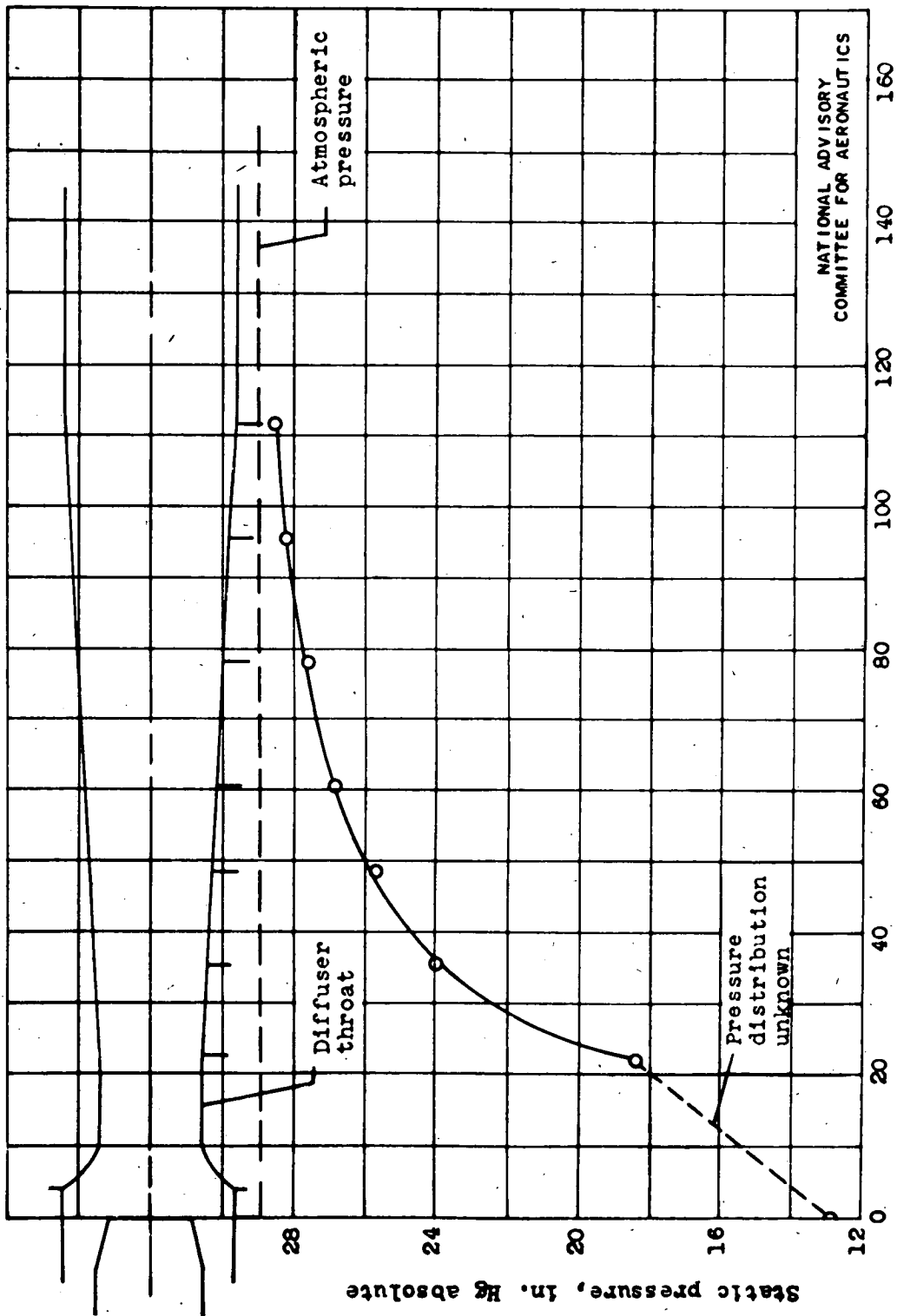


Figure 5. — Pressure distribution along diffuser with shutter full open. Corrected engine speed, 15,940 rpm.

Fig. 6

NACA RM NO. E6K29

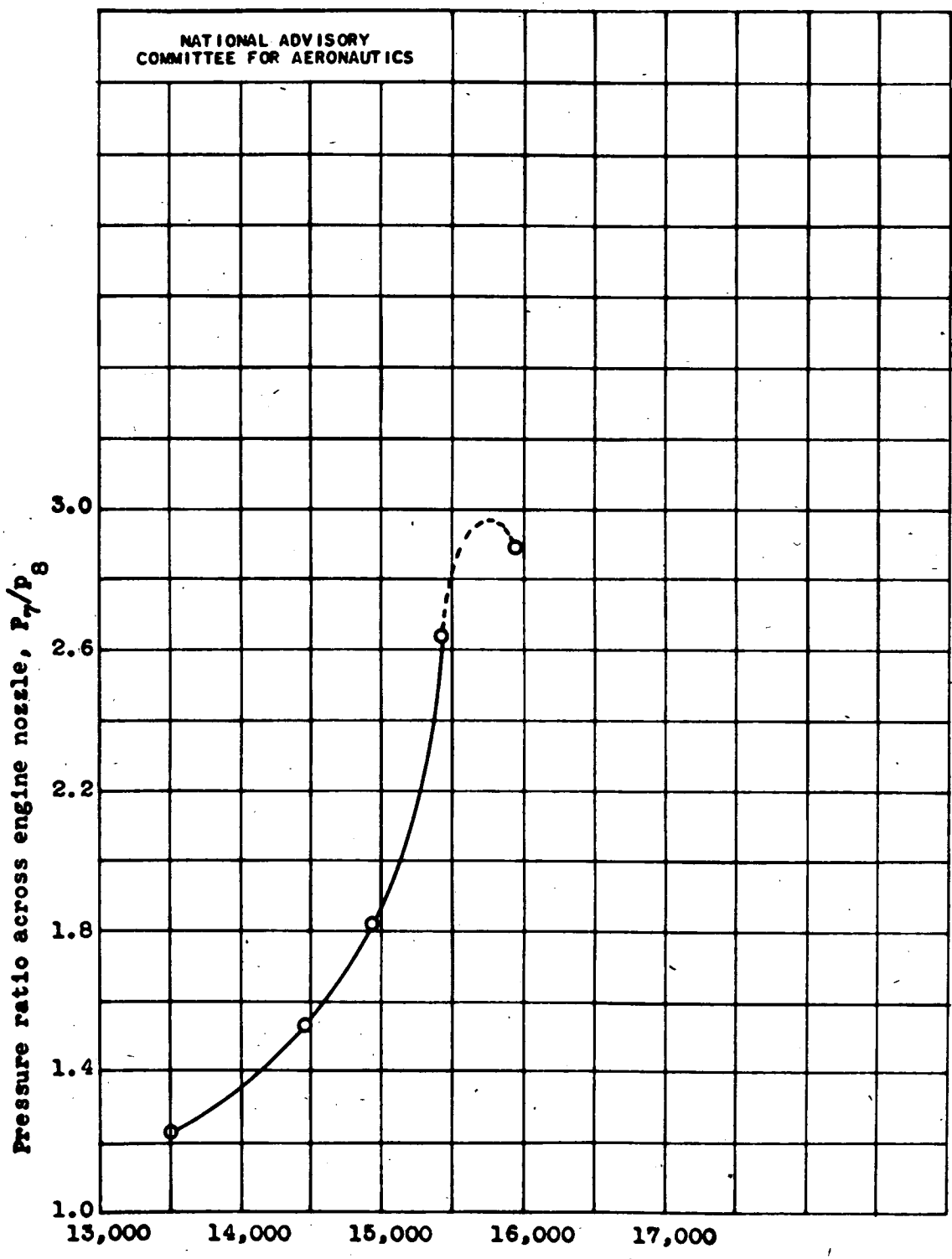


Figure 6. - Variation of pressure ratio across engine nozzle with corrected engine speed. Diffuser shutter, full open.

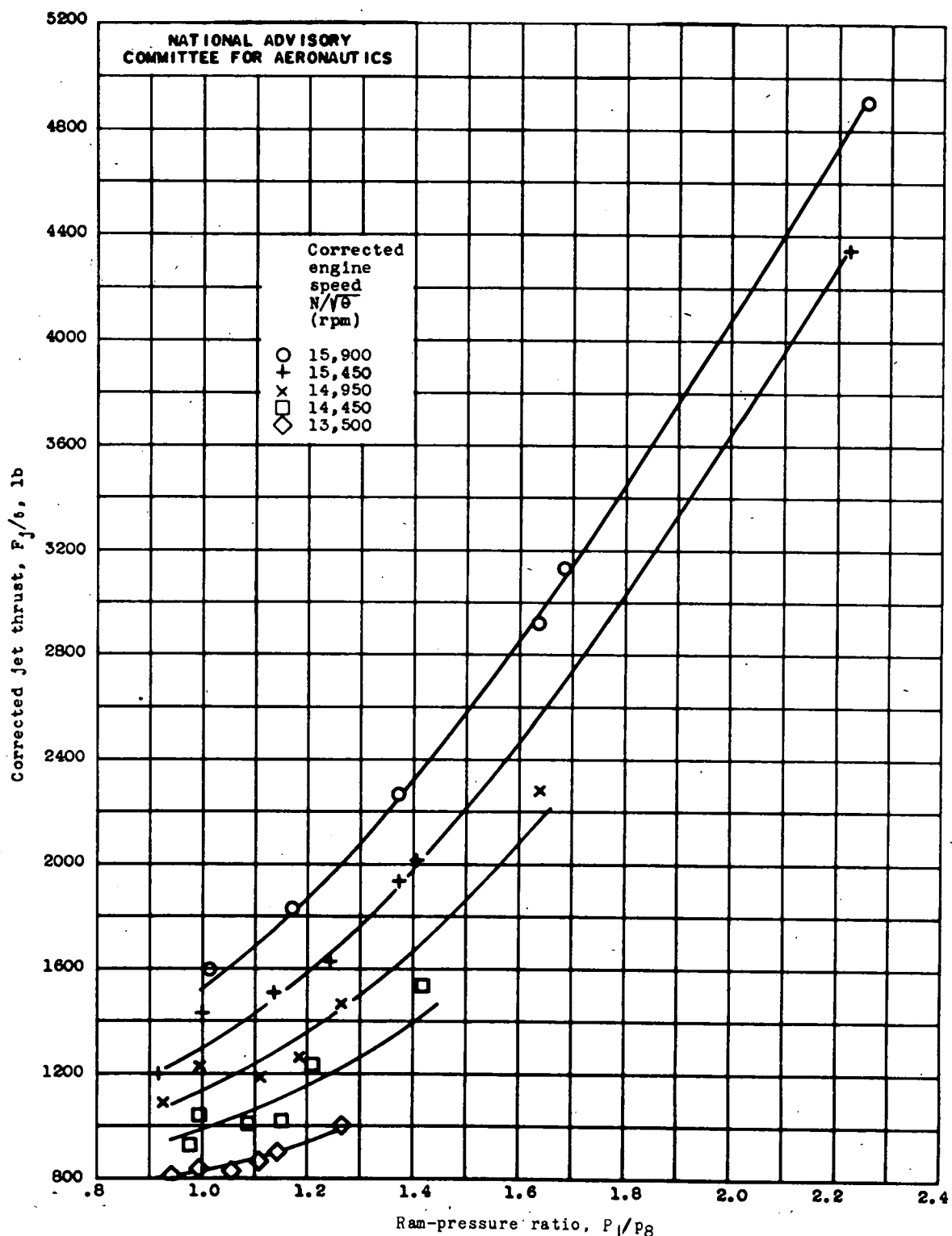


Figure 7. - Variation of jet thrust with ram-pressure ratio for various corrected engine speeds.

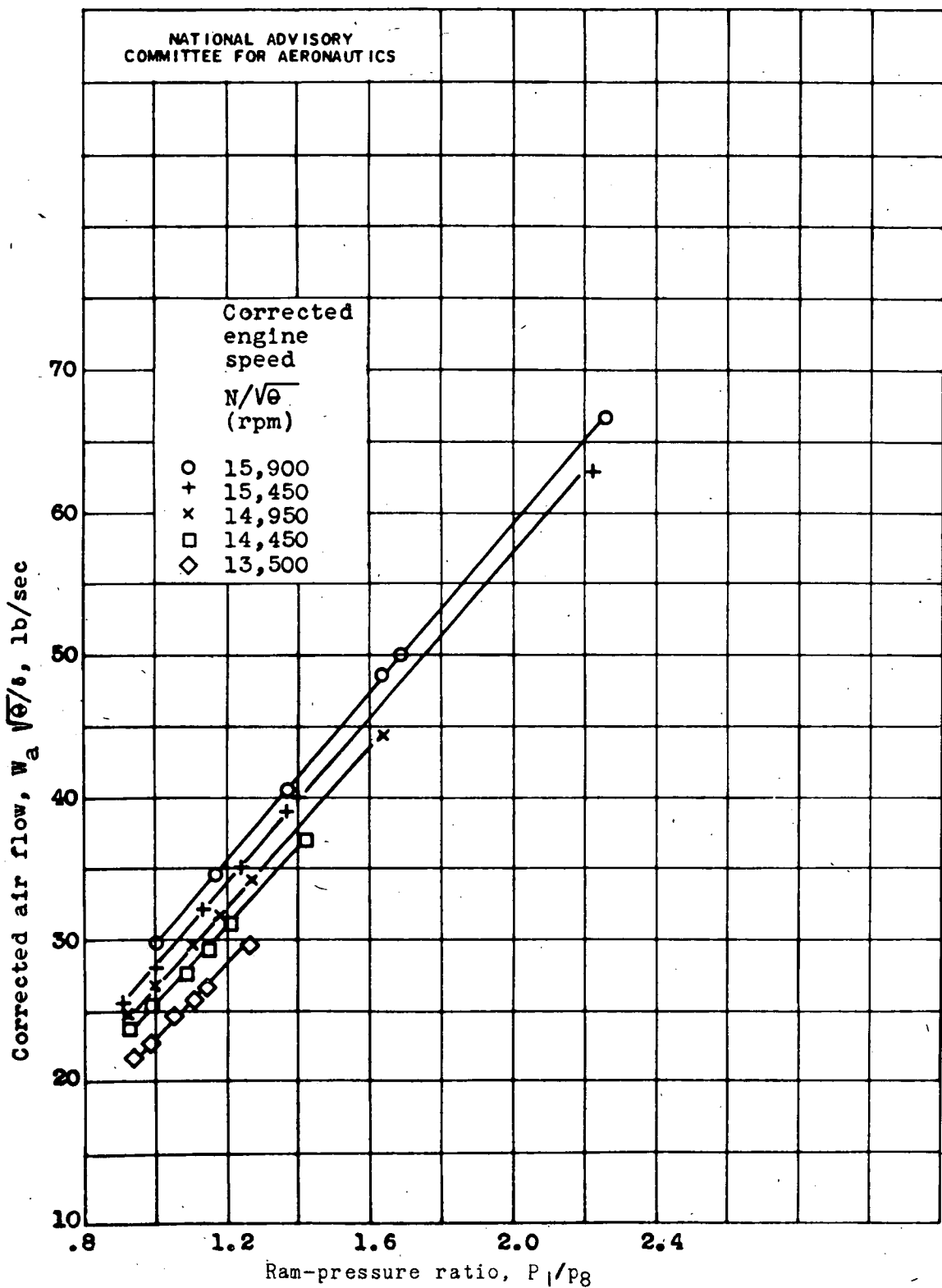


Figure 8. - Variation of air flow with ram-pressure ratio for various corrected engine speeds.

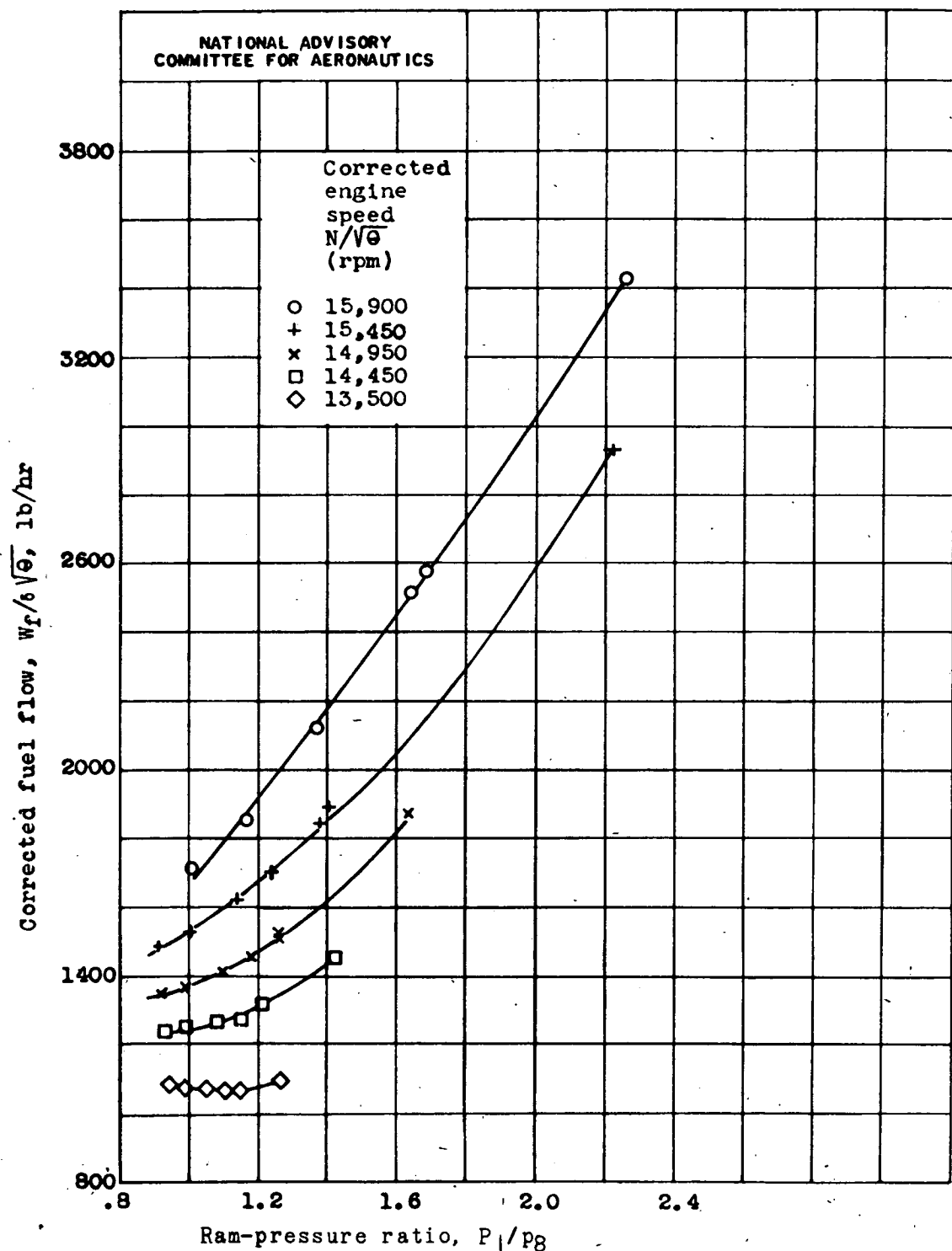


Figure 9.— Variation of fuel flow with ram-pressure ratio for various corrected engine speeds.

Fig. 10

NACA RM No. E6K29

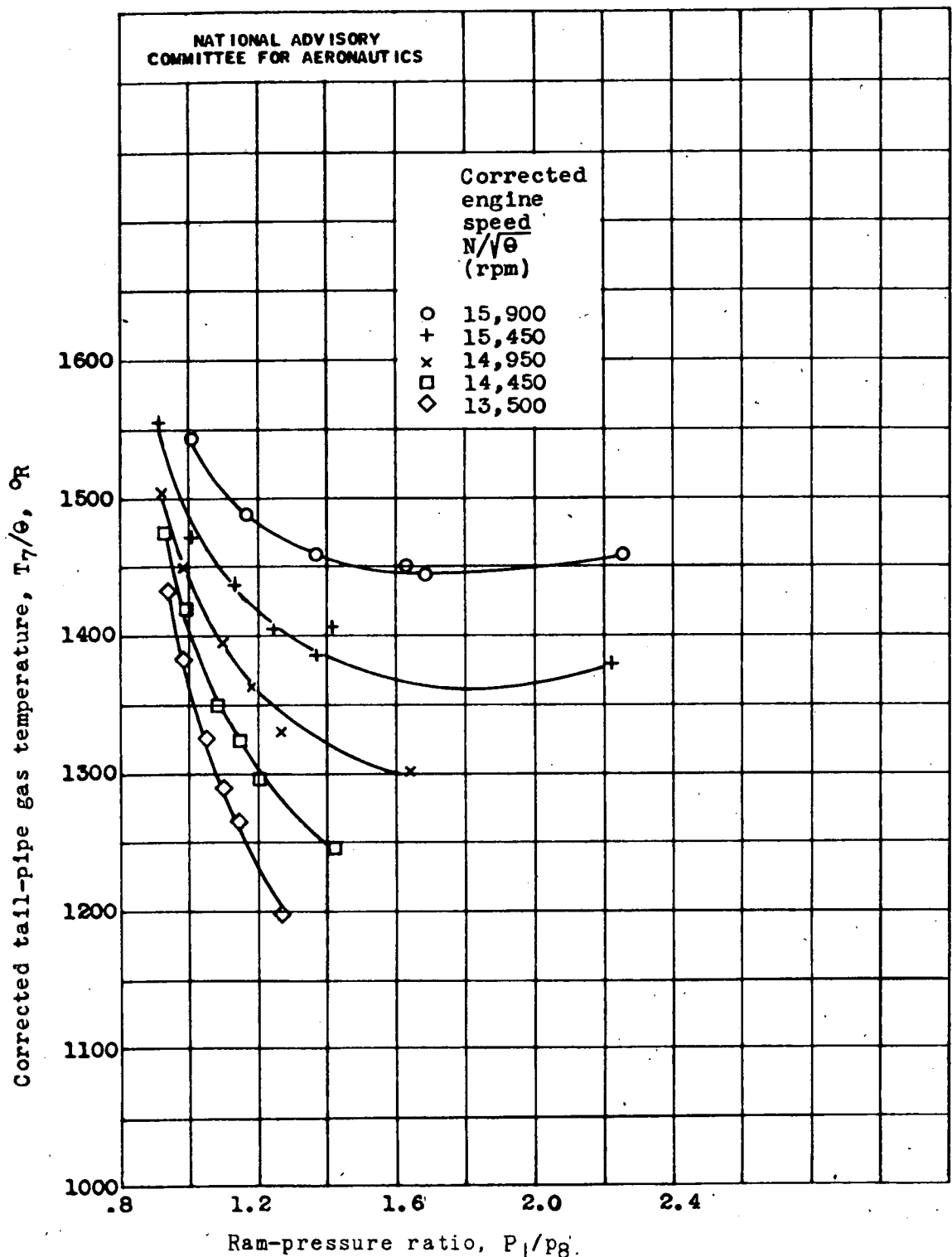


Figure 10. - Variation of tail-pipe gas temperature with ram-pressure ratio for various corrected engine speeds.

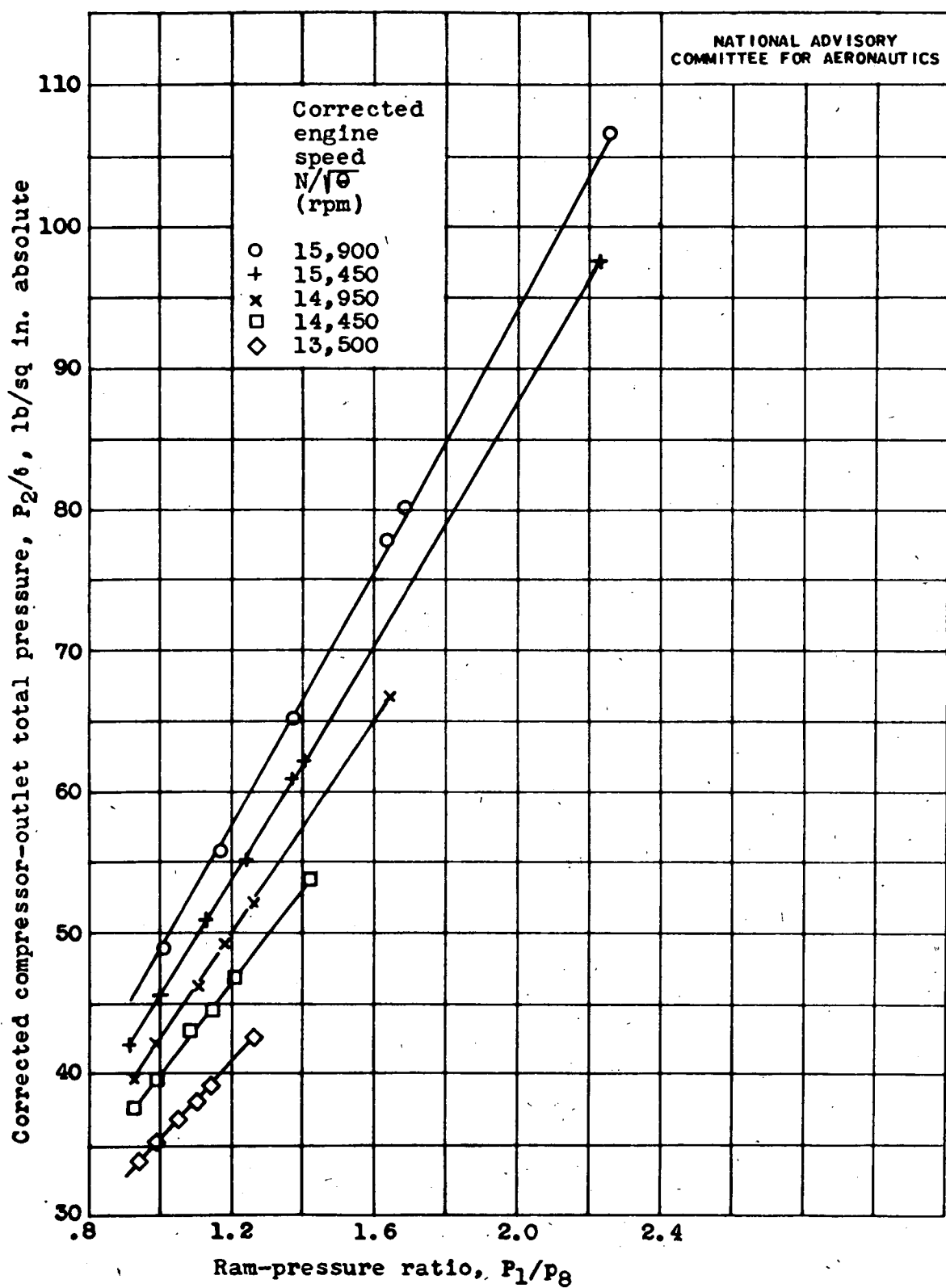
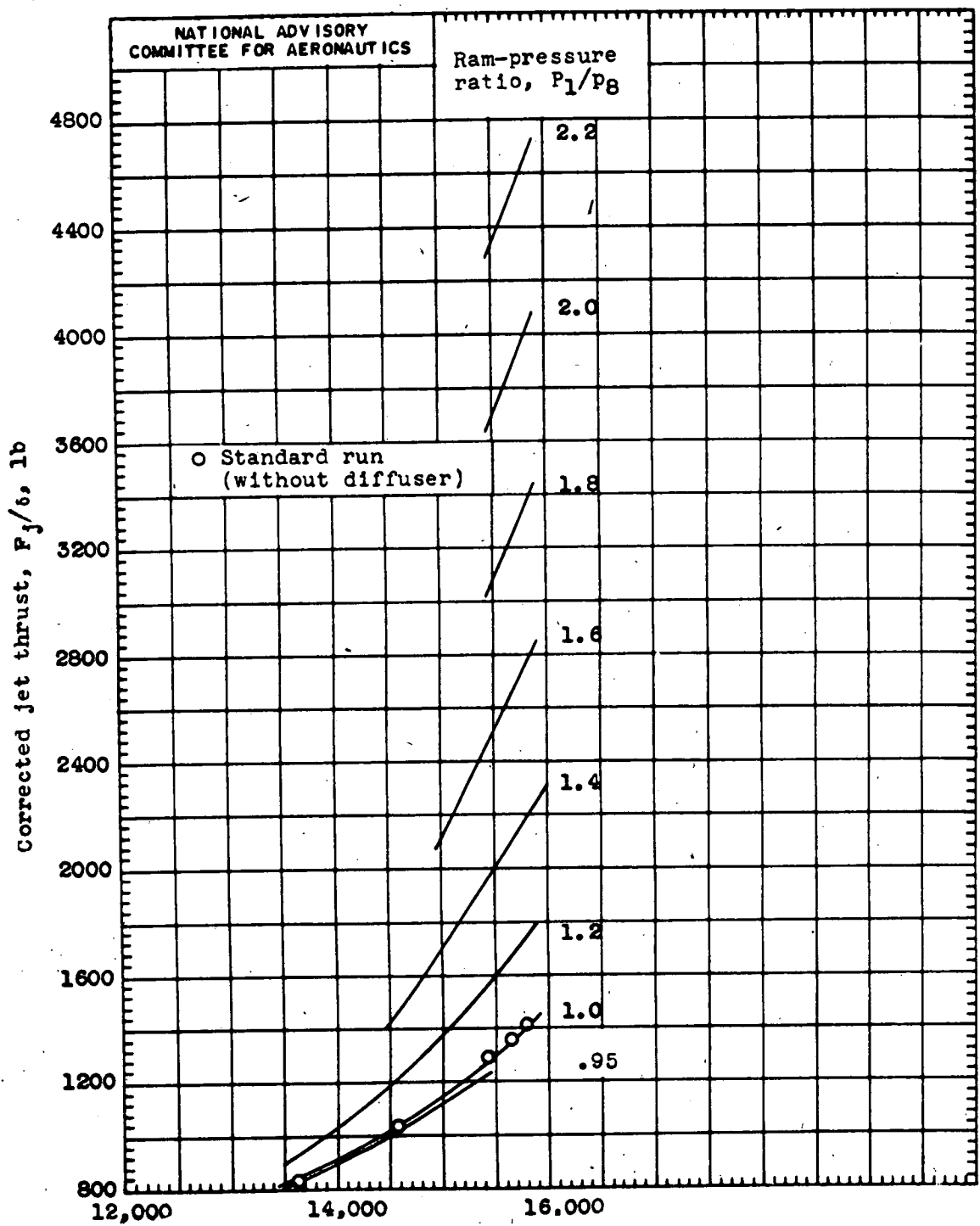


Figure 11. - Variation of compressor-outlet total pressure with ram-pressure ratio for various corrected engine speeds.



Corrected engine speed, $N/\sqrt{\theta}, \text{ rpm}$

Figure 12. - Variation of corrected jet thrust with corrected engine speed for various ram-pressure ratios.

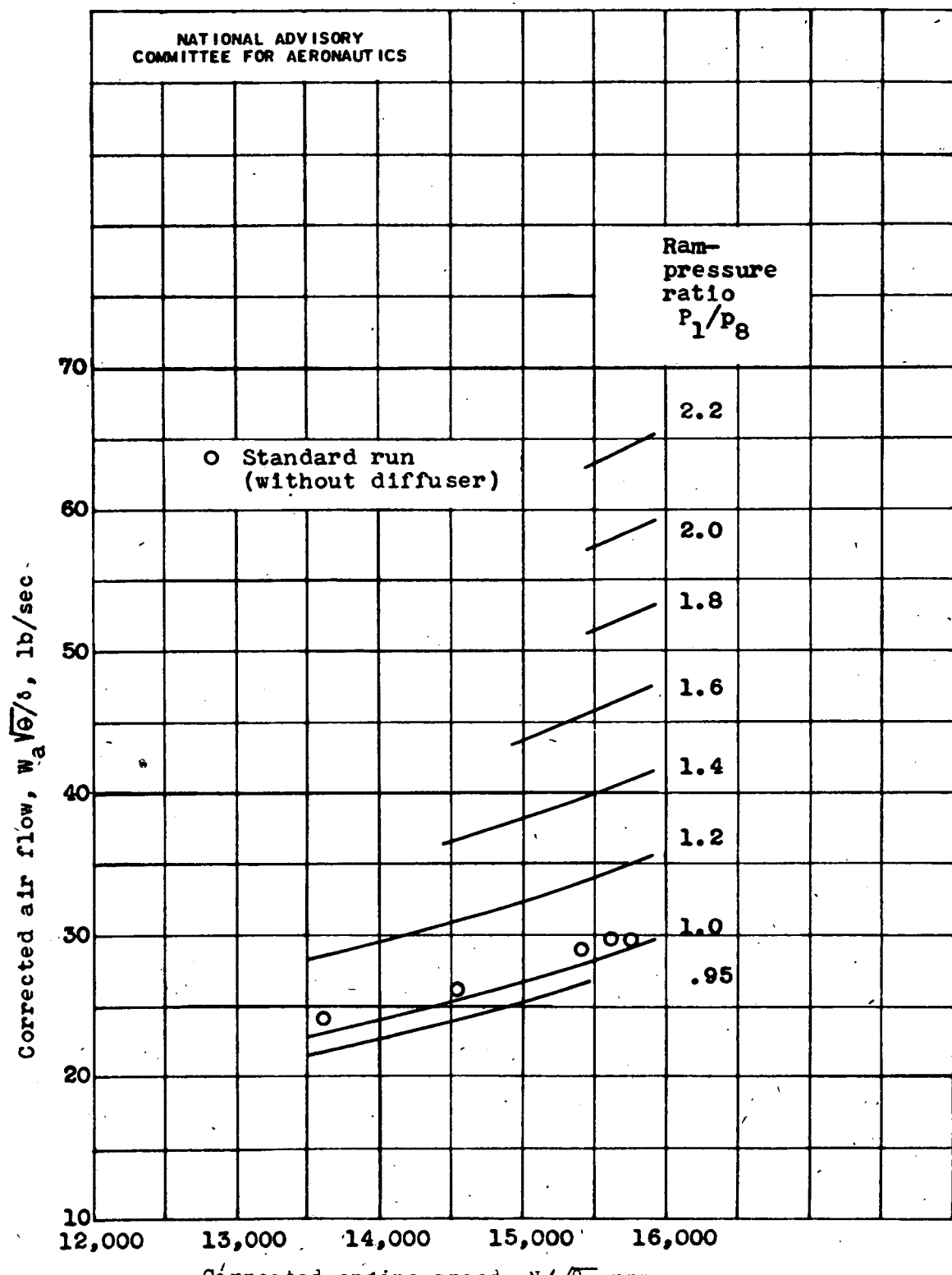


Figure 13: - Variation of corrected air flow with corrected engine speed for various ram-pressure ratios.

Fig. 14

NACA RM NO. E6K29

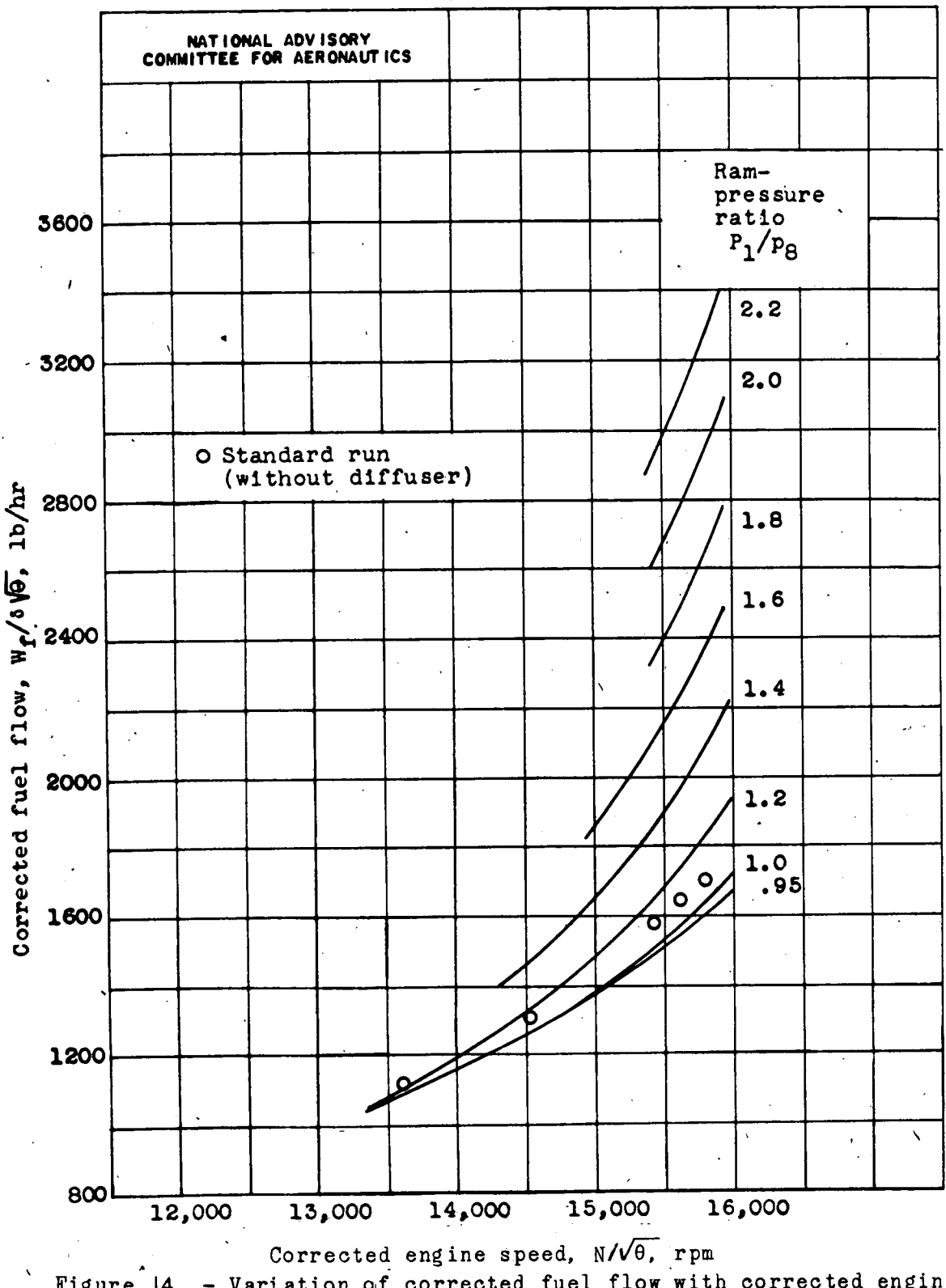


Figure 14. - Variation of corrected fuel flow with corrected engine speed for various ram-pressure ratios.

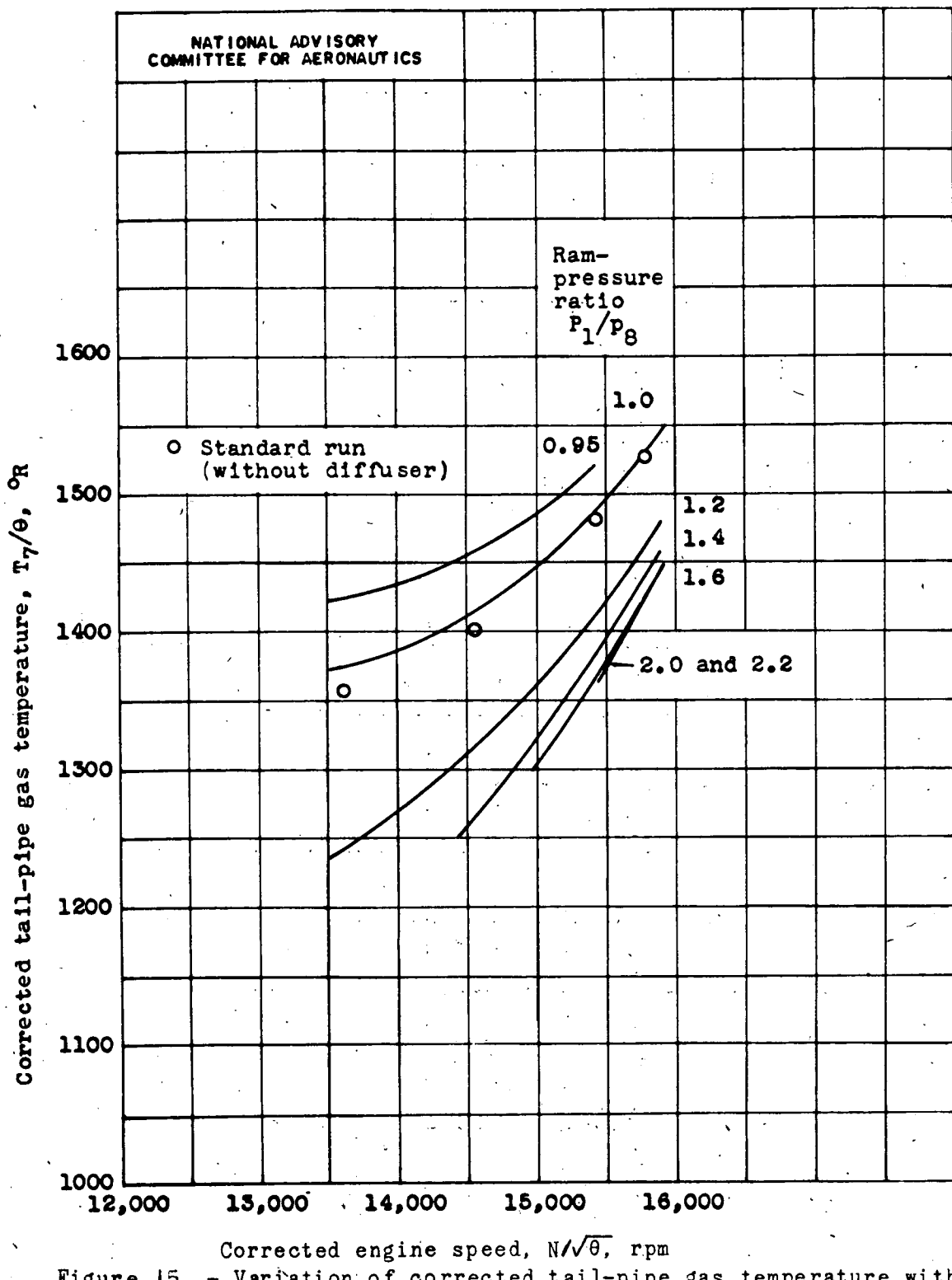


Figure 15. - Variation of corrected tail-pipe gas temperature with corrected engine speed for various ram-pressure ratios.

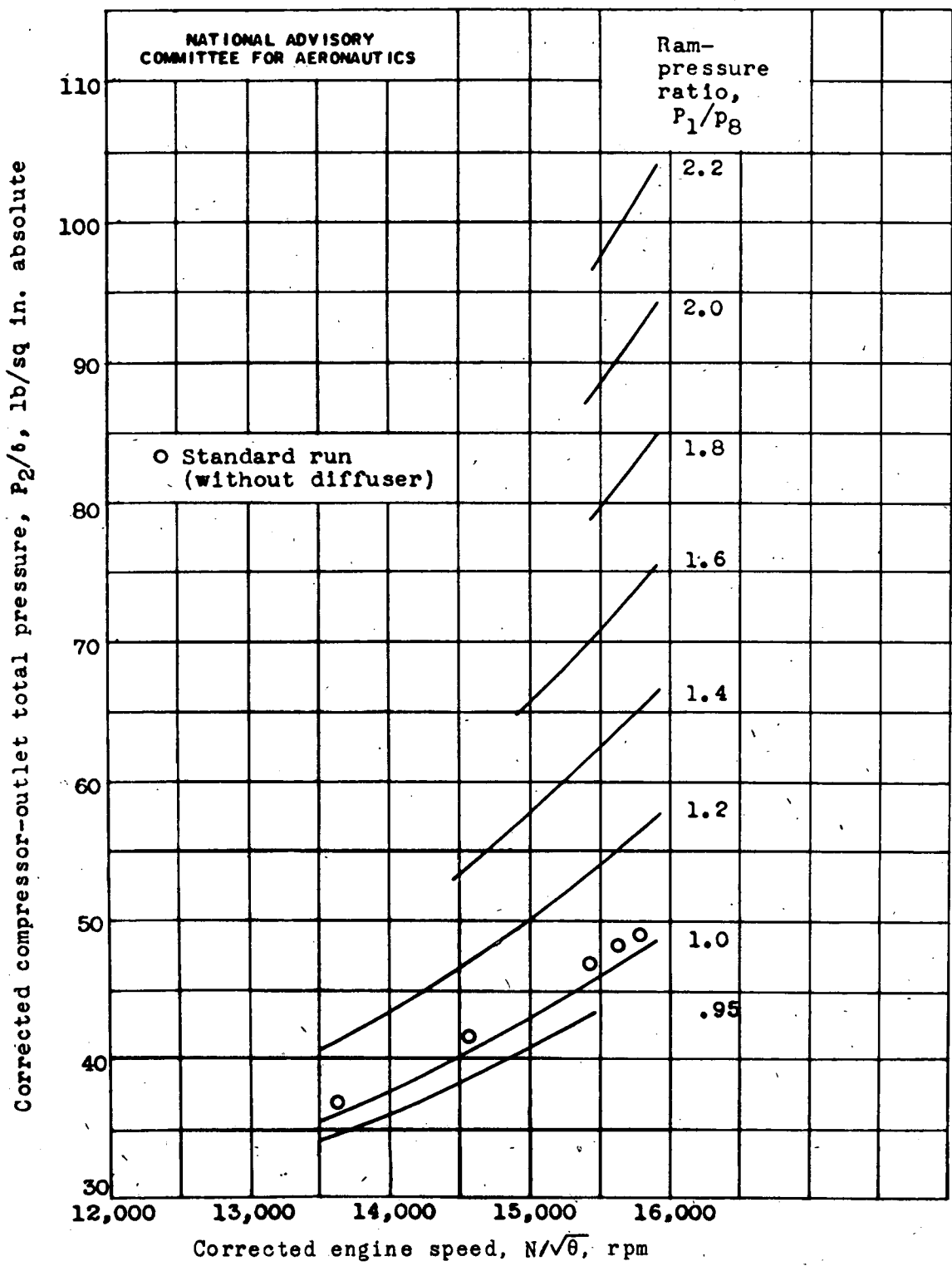


Figure 16. - Variation of corrected compressor-outlet total pressure with corrected engine speed for various ram-pressure ratios.

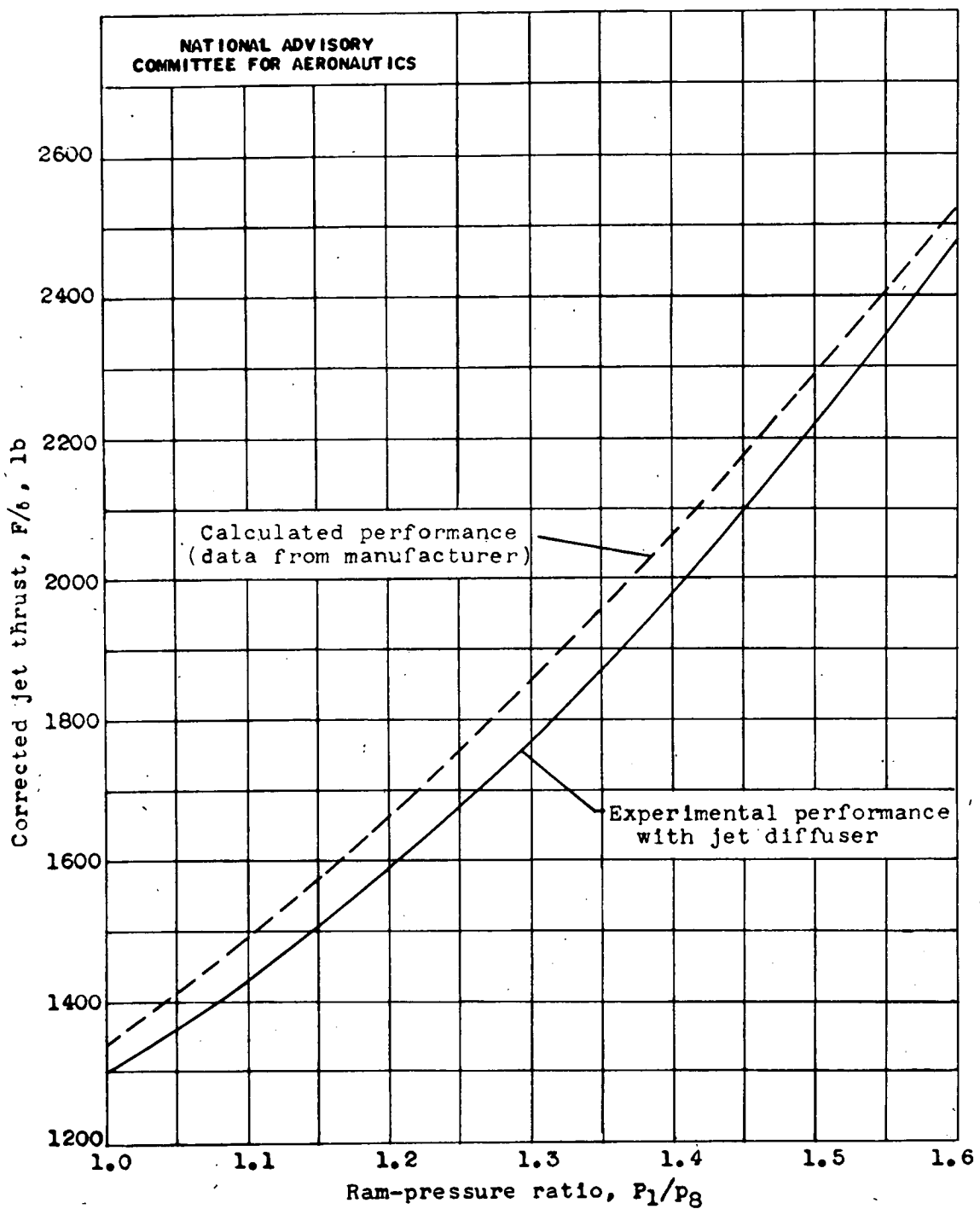


Figure 17. - Comparison of calculated performance with experimental performance obtained with jet diffuser. -Corrected engine speed, 15,450 rpm.